Short-range order in liquid matter probed by high-temperature x-ray absorption measurements

1996 J. Phys.: Condens. Matter 8 9335

(http://iopscience.iop.org/0953-8984/8/47/025)

J. Phys.: Condens. Matter **8** (1996) 9335–9339. Printed in the UK

Short-range order in liquid matter probed by high-temperature x-ray absorption measurements

Adriano Filipponi

European Synchrotron Radiation Facility, BP 220, 38043 Grenoble, France

Received 23 July 1996

Abstract. X-ray absorption spectroscopy can be applied to the study of liquid matter yielding quantitative structural information on the short-range order. Recent experimental advances and a new single-energy detection technique suitable for monitoring phase transition and supercooling phenomena are described. Examples of the change in absorption at the melting of Ge and Ag are presented. The general theoretical framework for the interpretation of the spectra is reviewed.

1. Introduction

X-ray absorption spectroscopy (XAS) [1] is a powerful structural technique to investigate the short-range order in condensed matter. The object of the measurement is the absorption coefficient around a deep-core-electron excitation edge from about 200 eV below up to about 1–2 keV above threshold. The photon absorption produces a photoelectron that probes the neighbourhood of the excited atom and, more precisely, the effective potential generated by the surrounding charges (nuclei and electrons). This interaction generates interference effects in the matrix element that are seen as oscillations in the absorption cross-section above the edge, called extended x-ray absorption fine structure (EXAFS). The intensity of these compound-dependent features, that contain the structural information, is of the order of 10% of the edge step, but can be as low as 1% in heavily disordered systems.

XAS is performed by measuring the x-ray absorption coefficient for a sequence of closely spaced energy points obtained scanning the monochromator angle. Experimental success requires a noise level in the absorption measurement in the 10^{-4} range and energy resolution not worse than $\Delta E/E \sim 10^{-4}$ to avoid instrumental broadening of edge features. Very important requirements are also the measurement reproducibility and both instrumental and source stability. Considerable additional difficulties are found in the case of experiments on liquid samples at high temperature where the need to produce a uniform $\sim$10 μm thick layer of molten substance in a basically containerless environment is far from trivial.

Several advances from the experimental and theoretical standpoint were made in recent times leading to the possibility of performing successful experiments on liquid matter and to obtain reliable structural information on the short-range order.

2. Experimental advances

A breakthrough in the experimental work was given by the idea of making homogeneous samples by dispersing sample powder into inert BN or graphite powder [2]. The mixture is

0953-8984/96/479335+05$19.50

pressed into a rigid pellet that supports the molten sample droplets when it is heated above the sample melting point T_m. While there are certain limitations concerning reactivity between sample and matrix or due to the environment characteristic this was found to be a very versatile technique applicable to a large class of systems including metals, semiconductors, binary alloys and molten salts. Measurements up to 3000 K under stationary conditions are performed using a high-temperature oven that operates in high vacuum (or controlled atmosphere) as previously described [2].

Major recent experimental advances come from the new XAS installations at third-generation sources like the European Synchrotron Radiation Facility (ESRF). In particular the bending magnet beamline BM29 at ESRF [3] is now equipped with automated cryostat and oven chambers covering a wide temperature range from 20 K to 3000 K.

Obvious advantages of the ESRF source are the exceptional stability and small vertical emittance. These characteristics allow one to have an excellent energy resolution and to rely on the reproducibility of the energy scale in subsequent spectra. This is essential for threshold measurements. In addition, the focusing capability [4] and the high flux allow one to collect excellent spectra also on small samples with useful size less than 1 mm. Recent applications are focused on the possibility of combining high-pressure and high-temperature conditions with a large-volume pressure cell [5]; the typical useful beam size is in this case 0.5 mm.

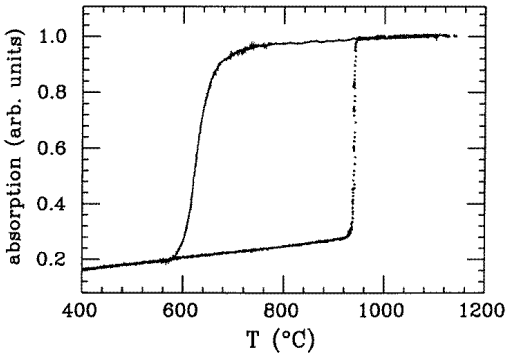

Figure 1. The single-energy x-ray absorption hysteresis loop obtained for a Ge sample at the K-edge inflection point while cycling the temperature above and below T_m. The supercooling phenomenon is quite evident.

The high-temperature experimental set-up at ESRF-BM29 is equipped with a combination of temperature probes (thermocouple and pyrometer) whose readout is directly integrated in the acquisition system. It is possible to perform various kinds of experiments including long acquisitions at constant temperature or successive short acquisitions at different temperatures. In addition, we have recently developed a novel experimental technique based on single-energy x-ray absorption detection performed while cycling the sample temperature in a wide range. This technique was found to be extremely useful to probe phase transitions and, in particular, melting and freezing thresholds under supercooling conditions. An example of such an experiment for pure Ge is shown in figure 1. The absorption coefficient is measured at the energy corresponding to the inflection point at the Ge K edge. Upon increasing the temperature a sudden increase of absorption is found at T_m, associated with the semiconductor to metal transition [6] occurring at the melting point. During the cooling process it is evident that the highly absorbing molten metallic

state persists down to nearly 700 °C. Quite remarkably the sample can be supercooled by nearly 300 K before crystallization takes place.

Complete EXAFS measurements suitable for structural analysis have been so far obtained for several systems including elemental metals like Ge, Pt, Ag, Rh, Sn, In [2, 6–10] molten salts [11–13] and binary alloys.

3. Theoretical framework

Several groups contributed to the development of the current theory for the EXAFS phenomenon [14, 15, 16] leading to equivalent formulations. The theory suitable for routine data analysis is based on (a) the one-electron, (b) dipole, and (c) muffin-tin approximations. The cross-section for the photoabsorption process is expressed by first-order perturbation theory as

$$\sigma(\hbar\omega) = 4\pi^2\alpha\ \hbar\omega \sum_f |\langle i|\hat{\epsilon}\cdot\boldsymbol{r}|f\rangle|^2\delta(E_f - E_i - \hbar\omega). \tag{1}$$

In the one-electron approximation the complicated many-electron wavefunctions are substituted by one-electron orbitals. For K edges the initial state $\langle i| = \langle 1\mathrm{s}|$ and the final state $|f\rangle = |\epsilon\mathrm{p}\rangle$ where the latter continuum wavefunction is calculated in a suitable effective potential. This potential takes into account the relaxation due to the core hole on the photoabsorber atom and the inelastic losses of the photoelectron through a complex energy-dependent exchange and correlation part [17] (Hedin–Lunqvist theory). The muffin-tin approximation consists in approximating this effective potential with a collection of spherically symmetrical potentials embedded in a constant-potential region and it leads to a simplification of the photoelectron scattering problem.

As a result of these approximations a certain number of empirical parameters have to be introduced and adjusted to optimize the agreement with experiment. These are the energy shift between theoretical and experimental scales E_0, an overall amplitude reduction factor S_0^2, and the atomic background. The latter contains features associated with double-electron excitation edges that can be empirically modelled and calibrated on model compounds [18].

It should be noted that XAS is sensitive to the effective potential for the photoelectron that is generated by both nuclear and electronic charges. Therefore its sensitivity is somewhere in between with respect to neutron and x-ray diffraction, which probe nuclei and electronic charge density respectively. In practice, however, the signal is dominated by the deep scattering centres of the nuclear positions.

Our applications of the XAS technique to probe the local structure of liquid matter are based on a quite general formulation in which the connection between the n-body distribution functions and the structural signal is made transparent [19]. This formulation is based on a decomposition of the structural signal into irreducible n-body terms:

$$\chi(k) = \sum_i \gamma^{(2)}_{(0,i)}(k) + \sum_{(i,j)} \gamma^{(3)}_{(0,i,j)}(k) + \sum_{(i,j,k)} \gamma^{(4)}_{(0,i,j,k)}(k) + \cdots. \tag{2}$$

The $\gamma^{(n)}$-signals can be calculated by means of an efficient continued-fraction expansion technique [20], and can be averaged over n-particle distribution function using various formulas according to the level of disorder. In the general case of single-component systems the configurational average of the signals is given by

$$\langle\chi(k)\rangle = \int_0^\infty \mathrm{d}r\ 4\pi r^2\rho g_2(r)\gamma^{(2)}(r,k) + \int \mathrm{d}r_1\ \mathrm{d}r_2\ \mathrm{d}\phi\ 8\pi^2 r_1^2 r_2^2 \sin(\phi)\rho^2 g_3(r_1, r_2, \phi)\gamma^{(3)}(r_1, r_2, \phi, k) + \cdots. \tag{3}$$

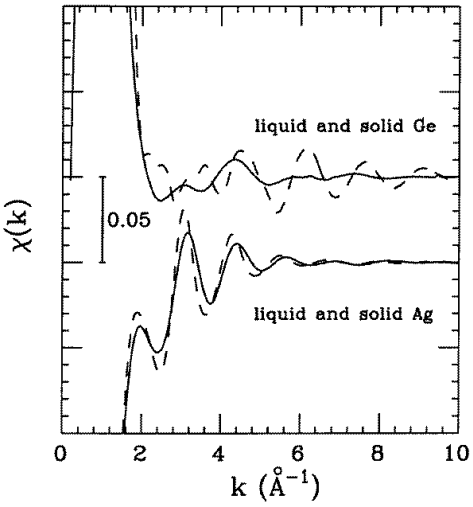

Figure 2. The difference between the EXAFS spectra of solid (dashed lines) and liquid (solid lines) specimens in the neighbourhood of T_m for Ge and Ag. In the latter case the similarity of the short-range environment induces only small changes in the absorption. In Ge instead there is a dramatic change in coordination and conductive properties.

The successive terms have a decreasing importance but contributions from the three-body signal (second integral) are often seen. While the extension of the integration formally extends to infinity there are exponential cut-off terms in the γ-signals that limit the actual EXAFS sensitivity to the short range.

Striking experimental evidence for this characteristic is given in figure 2 where the threshold features of crystalline and molten specimens are compared on a magnified scale. In the case of Ag only a weak change occurs upon melting. This is due to the substantially unaltered short-range environment from the f.c.c. solid to the close-packed liquid structure. Larger differences are instead observed when melting is accompanied by a drastic change in the local structure like in the Ge case [6]. In any case there is no specific signature for the onset of long-range crystalline order comparable to the powder diffraction rings for instance. The lack of long-range-order sensitivity allows one to perform the same experiment and apply the same data analysis on any condensed form of the substance including crystalline and liquid phases as a function of temperature.

The structural information is usually retrieved in the form of distances and coordination numbers for a series of neighbouring shells. In the case of a liquid system the short-range sensitivity poses severe problems since there is not enough information to determine the full $g(r)$. Contrary to what is commonly believed knowledge of low-k data does not improve the situation. There is no analogy between the information contained in the low-q region of the structure factor $S(q)$ from diffraction measurements and the equivalent of $\chi(k)$. Due to the lack of long-range information the adoption of a simple peak-fitting procedure for $\chi(k)$ may result in erroneous determinations. It is therefore necessary to combine the short-range structural information from the $\chi(k)$ with external information on the long-range order. We have proposed a simple constrained fitting procedure [8] based on model refinement. Only the long-range $g(r)$ tail and the compressibility limit of the corresponding $S(q)$ are retained from the model, while the short-range shape is refined with a usual peak-fitting procedure.

The model can be taken from previous diffraction data, computer simulation or can even be a very simple approximation like a hard-sphere fluid. This constrained procedure has been widely applied yielding realistic $g(r)$-shapes in several cases [6, 7, 8].

4. Conclusions

While XAS applications to solid matter are well established, recent research efforts demonstrated the feasibility and reliability of investigations on liquid matter. XAS was shown to be a quantitative structural technique sensitive to the short-range order. The complementarity with diffraction measurements has been emphasized and efforts to combine the experimental data encouraged. These results justify the development of long-term research projects for the investigation of elemental and binary fluids in a wide range of thermodynamic conditions, including supercooled metastable states. The availability of high-brilliance third-generation sources is currently opening new possibilities due to the improved data quality and the development of novel detection techniques.

Acknowledgments

The present research is a result of a long-standing collaboration with A Di Cicco (Camerino, Italy); the experimental activity has been carried out at the LURE (Orsay, France) D42-D44 beamline and is now continuing at ESRF (Grenoble, France) BM29. Invaluable help from the staff of these laboratories is acknowledged.

References

[1] Koningsberger D C and Prins R 1988 *X-ray Absorption: Principles, Applications, Techniques of EXAFS, SEXAFS, and XANES* (New York: Wiley)
[2] Filipponi A and Di Cicco A 1994 *Nucl. Instrum. Methods* B **93** 302
[3] Mason R (ed) 1995 *E.S.R.F. Beamline Handbook* (Grenoble: E.S.R.F.)
[4] Müllender S, Marion P, Zhang L, Brookes N B and Goulon J 1995 *Physica* B **208+209** 225
[5] Besson J M, Nelmes R J, Hamel G, Loveday J S, Weill G and Hull S 1992 *Physica* B **180 & 181** 907
[6] Filipponi A and Di Cicco A 1995 *Phys. Rev.* B **51** 12 322
[7] Di Cicco A 1996 *Phys. Rev.* B **53** 6164
[8] Filipponi A 1994 *J. Phys.: Condens. Matter* **6** 8415
[9] Filipponi A and Di Cicco A 1995 *Phys. Rev.* A **52** 1072
[10] Di Cicco A and Filipponi A 1996 *Proc. 9th LAM conference (Chicago, 1995); J. Non-Cryst. Solids* **205–207** at press
[11] Di Cicco A, Minicucci M and Filipponi A 1996 submitted
[12] Di Cicco A, Rosolen J M, Marassi R, Tossici R, Filipponi A and Rybicki J 1996 *J. Phys.: Condens. Matter* accepted
[13] Di Cicco A 1996 *J. Phys.: Condens. Matter* **8** 9341
[14] Benfatto M, Natoli C R, Bianconi A, Garcia J, Marcelli A, Fanfoni M and Davoli I 1986 *Phys. Rev.* B **34** 5774
[15] Gurman S J, Binsted N and Ross I 1986 *J. Phys. C: Solid State Phys.* **19** 1845
[16] Mustre de Leon J, Rehr J J, Zabinsky S I and Albers R C 1991 *Phys. Rev.* B **44** 4146
[17] Tyson T A, Hodgson K O, Natoli C R and Benfatto M 1992 *Phys. Rev.* B **46** 5997
[18] Filipponi A 1995 *Physica* B **208+209** 29
[19] Filipponi A, Di Cicco A, Tyson T A and Natoli C R 1991 *Solid State Commun.* **78** 265
Filipponi A, Di Cicco A and Natoli C R 1995 *Phys. Rev.* B **52** 15 122
Filipponi A and Di Cicco A 1995 *Phys. Rev.* B **52** 15 135
[20] Filipponi A 1991 *J. Phys.: Condens. Matter* **3** 6489